Experimental Characterization of Particle Swarm Optimized Focusing Non-Uniform Grating Coupler for Multiple SOI Thicknesses

Luca Zagaglia, Francesco Floris, and Peter A. O'Brien

***Abstract*—We report the first experimental characterizations of the coupling efficiencies of a series of e-beam fabricated focusing non-uniform grating couplers interfaced with a horizontal fiber coupling-scheme and designed for multiple Silicon-On-Insulator thicknesses, spanning between the 220 and 340 nm standard platforms. The design of nonuniform grating couplers is tackled either from an engineering perspective focused on to the optimization of the structures for this particular coupling-scheme; and a physics perspective related to the investigation of the scattering process of each structure for a complete comprehension of its performance in support to the experimental findings. Measured coupling efficiencies, up to 83% for the 340 nm platform at 1550 nm, are reported showing to be in excellent agreement with the theoretical findings. The physics behind the scattering process of each structure is investigated taking advantage of the Finite Difference Time Domain method to obtain a deeper understating of the coupling efficiencies. Consequently, a new parameter, the integrated leakage factor, together with the variation of the effective refractive index, across the local pitches, are calculated. Our belief is that any coupling structure for grating coupling can benefit from the proposed designed approach, as a widely applicable technique.**

***Index Terms*—Computational optimization algorithms, coupling efficiency, focusing non-uniform grating couplers, optical fibers.**

I. Introduction

Silicon Photonics has been one of the major topic for more than a decade stimulating the interest of scientists either from a fundamental and an applied researcher prospective [1]. In this framework, two different approaches are characterizing the studies: one more oriented on the optimization and the performances of the photonics structures and a second focused on the innovation and the propose of new optical devices. The primary driving force behind Silicon photonics is represented by the combination of the properties of the material and the practical experience of processing high-volume, low-cost electronics over the years. Nowadays, the increasing need for smaller and high-performance Photonics Integrated Circuits (PICs) has supported research related to Silicon-on-Insulator (SOI) architecture, a leading platform for cutting-edge technological applications [2]. The key features of the SOI platform are the small feature size due to the high refractive index contrast enabling a strong light confinement and the compatibility with the well-established CMOS technology allowing for the integration with the electronic integrated circuits [3]–[4]. Currently, one acknowledged challenge is the optimization and fabrication of optical connections between the microscopic features of the components integrated on the PIC and the dimensions of fiber-optic connections. The main goal is to maximize the Coupling Efficiency (CE) while matching the different mode sizes of the different structures in use [5].

Grating couplers (GCs) represent a promising solution due to the possibility of placing these structures almost anywhere on the PIC, while providing relatively relaxed alignment tolerances compared to competing edge-coupling geometries [6]–[7]. A wide variety of GCs structures have been optimized for the 220 nm and 340 nm-thick SOIs standard platforms [8]–[10]; in particular, on a "pure" SOI platform, non-uniform GCs (characterized by a non-constant pitch) have been demonstrated as the highest performers displaying theoretical and experimental CE values up to 89 and 81% respectively [11]–[17].

The majority of non-uniform GCs have been optimized in the vertical geometry through a Vertical Fiber coupling-scheme (V-Fb), Fig. 1 panel (a). While the V-Fb is useful for probe-testing and simple to model using computational methods, it does not represent an optimum form-factor for packaging PICs into photonic devices due to the fragility of glass. Due to its improved mechanical stability and form-factor advantageous when packaging photonic devices, a Horizontal fiber scheme (H-Fb), Fig. 1 panel (b), can be a valid alternative. In fact, its planarity allows to reduce the vertical dimension of the final package resulting in a less bulky photonic device typical of an almost 2D structure [6].

However, due to the complexity in modelling this coupling-scheme, studies are limited representing a chance for novel research. In fact, this horizontal scheme involves simulating a relatively large cross-section (100 x 100 um) rather than the vertical scheme (10 x 10 um).

Thus, the characterization of new structures enabling the access to this coupling-scheme represent a challenging and stimulating opportunity, and incidentally state-of-the-art solutions

Manuscript received February 12, 2021; revised April 23, 2021; accepted May 8, 2021. Date of publication May 12, 2021; date of current version August 2, 2021. This work is supported in part by the Scientific Foundation Ireland under the Grant SFI-12/RC/2276_P2. *(Corresponding Author: Luca Zagaglia.)*

The authors are with Tyndall National Institute, Lee Maltings Complex Dyke Parade, Cork, Ireland T12 R5CP (e-mail: luca.zagaglia@tyndall.ie; francesco.floris@tyndall.ie; peter.obrien@tyndall.ie).

This article has supplementary material provided by the authors and color versions of one or more figures available at https://doi.org/10.1109/JLT.2021.3079575.

Digital Object Identifier 10.1109/JLT.2021.3079575

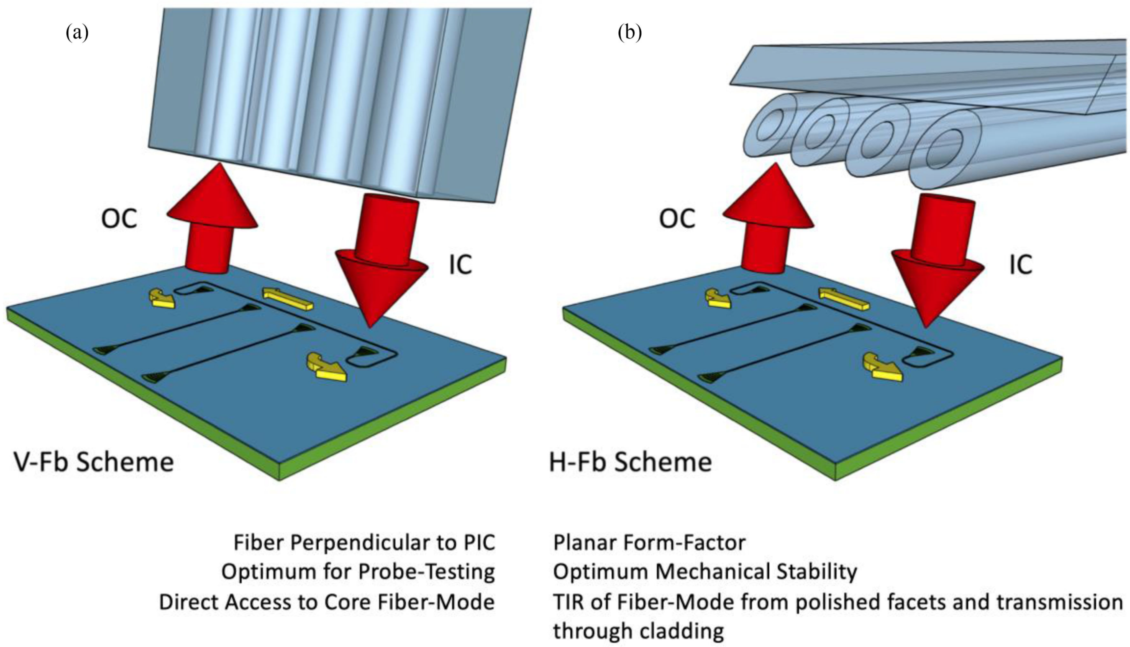

Fig. 1. Sketches of the measuring geometries. (a) Vertical fiber (V-Fb) scheme for light-coupling. (b) Horizontal fiber (H-Fb) scheme for light-coupling. The light (shown as red arrows) is injected into the chip via the input-channel (IC) and collected using the out-channel (OC).

for integrated photonic may benefit from this [18]. In this frameworks, non-uniform GCs are one of the most promising options and therefore the optimization of such structures represents the logical step to pursue.

In this work, we propose for the first time a complete state-of-the-art procedure, from the design to the experimental characterization, of optimized focusing non-uniform GCs for multiple SOI thicknesses (220 nm, 260 nm, 290 nm, 320 nm, and 340 nm) interfaced with a H-Fb displaying values of CEs competitive with the well-established V-Fb scheme. Accordingly, we study the behavior of the CEs as a function of the SOI thicknesses with particular attention on the variation of the scattering strength for higher Silicon thicknesses through the study of a new parameter called integrated leakage factor, α_{int}. In addition, the effect of the non-uniformity of the pitch on the propagation of the light is analyzed evaluating the effective refractive index estimated resorting to a photonic band structure analysis. We believe that our approach in designing focusing non-uniform GCs for H-Fb is a widely applicable technique and can be further generalized to any coupling structure for grating coupling.

II. Design and Experimental method

The non-uniformity of the GCs is the starting point of the design process taking advantage of a linear apodization function of the filling factor along the apodization direction (*X*)

$$FF(X) = FF_0 - AX \tag{1}$$

where FF_0 is the initial filling factor and *A* is the linear apodization factor as previously reported in the design rule developed by Marchetti *et al.* [12]. Then, the local pitch P_i is tuned using the well-known Bragg Law

$$P_i(X) = \frac{\lambda_c}{n_{eff}^{AVG}(FF, ED, X) - n_{SiO_2} * \sin(\theta_{in})} \tag{2}$$

where $\lambda_c = 1550$ nm is the tuning wavelength, $\theta_{in} = 10$deg the incident angle, and $n_{SiO2} = 1.44$ the background index, and $\mathrm{n_{eff}^{AVG}}$ is the averaged effective refractive index, which depends on *FF*, *X*, and the etching depth (*ED*). The mismatch in the Bragg-condition due to the approximate estimation of n_{eff}^{AVG} was corrected through an iterative process, as reported by Passoni *et al.* [19], leading to an additional parameter called mismatch compensation factor (*a*).

The H-Fb has been built inside Lumerical FDTD [20], a commercial Finite Difference Time Domain (FDTD) software, enabling us to obtain a complete representation of the fiber emission. The latter, being Gaussian, can be described by a unique angle of divergence enabling to exploit 2D-FDTD simulations to capture its mode field diameter (MFD) at the bottom interface between the fiber cladding and the PIC top-oxide layer. This allows us to build a corresponding Gaussian source mimicking the H-Fb emission avoiding huge FDTD simulation area, consequently reducing dramatically the simulation time.

A home-made design routine based on a customized particle swarm algorithm has been developed due to its simple mathematical structure based on one unique operator, as reported in [21], resulting in an easy implementation inside an external computational method, such as the FDTD.

The design routine is used to optimize $\mathrm{FF_0}$, A, and ED, and consequently the $\mathrm{P_i}$, in order to maximize the CE of the set of non-uniform GCs under investigation [22]. The top-oxide layer (TOX) thickness is not a parameter optimized through the design routine, as an index-matching epoxy filler is used during the measurement process to fill the air gap between the TOX facet and

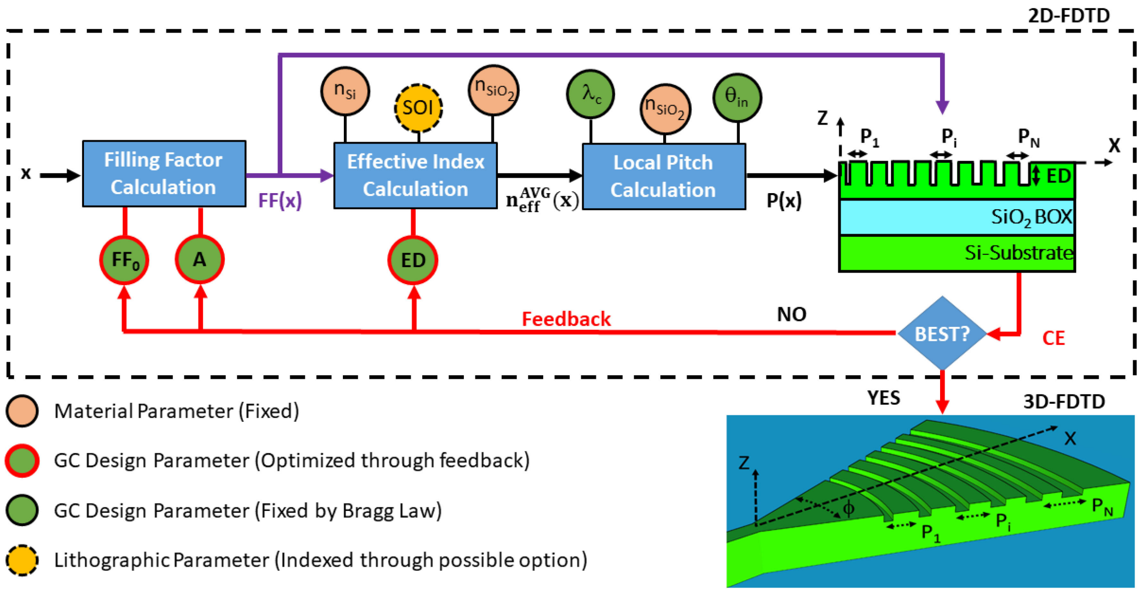

Fig. 2. Process flow diagram used to optimize the non-uniform grating coupler (GC) structures.

TABLE I
PARTICLE SWARM OPTIMIZED PARAMETERS OF THE GRATING COUPLER DESIGNS FOR EACH SOI THICKNESS

SOI Thickness (nm)	Etching Depth ED (nm)	Initial filling factor FF_0	Linear apodization factor A (nm^{-1})	Mismatch compensation factor a
220	94	0.9	27477E-9	1.0019
260	133	0.9	27072E-9	1.0158
290	176	0.9	27162E-9	1.0237
320	189	0.9	28369E-9	1.0228
340	209	0.9	28369E-9	1.0238

the fiber-array cladding. Finally, three dimensional simulations (3D-FDTD) are used to optimize the adiabatic tapering process [23] resulting in the best focusing angle $\phi = 40°$ for all the SOI thicknesses. A visual representation of the optimization process flow is depicted in Fig. 2 and the best parameters for the different SOI thicknesses under investigation are reported in Table I.

An Alienware Area 51 (Dell) with a liquid-cooled Intel Core processor i9-7960X (16 core, 32 threads) and 64GB of RAM is used to perform the design routine.

With this hardware architecture, the algorithm requires approximately 2 hours to optimize the design of one grating coupler, a single 2D-FDTD simulation takes few second to be completed, while a 3D-FDTD simulation of the optimized design needs 4 hours.

Through the services offered by Cornerstone, the open source silicon photonics foundry at the University of Southampton [24], the optimized structures were realized using the e-beam lithography, which ensures an adequate resolution at the nanometer scale to resolve the tiny and narrow trenches proper of these non-uniform GCs. Multiple samples of the same structures were fabricated introducing deliberate constant biases during the exposure processes to overcome potential deviations from the nominal simulated parameters due to fabrication tolerances. The waveguide propagation losses were also measured resorting to specific additional spiral structures.

The detailed layout of the fabricated chip is reported in supplementary material section 1 Fig. 1S.

A campaign of systematic broadband-transmittance measurements was performed to collect the CEs for all the samples using a customized auto-aligner machine to actively align the H-Fb array respect to the input- and output channel on the PIC. Further details on the measurement set-up can be found in supplementary material section 1.

III. RESULTS AND DISCUSSION

The best measured CE together with the theoretical counterparts for each SOI thickness are shown in Fig. 3.

For the first time experimental results are also shown together with the computational optimized one and as displayed, the two frameworks are in excellent agreement with an average difference of about 3% between the corresponding CEs. Moreover, the 2D FDTD values are comparable with the results of a similar analysis reported in literature for a V-Fb scheme [11]. A 5% reduction respect to the published CEs is reasonable considering a lower scattering strength displayed by our structures optimized for a wider MFD proper of a H-Fb scheme.

Also, the agreement between the 3D and 2D model is better than 95%. This decreasing can be brought back to a sensitivity dependence with respect to the mesh accuracy that limits the sampling of the curvature teeth of the focusing GCs. The higher disagreement at thicker Silicon thicknesses can be due to a greater quantity of material that is under-sampled. It is worthy to highlight that the best CEs of 56% and 83% has been measured respectively for the 220 nm- and the 340 nm-thick standard SOI platforms showing the competitiveness of the H-Fb scheme with the CEs related to the well-established V-Fb scheme [13]–[14]. A quadratic fit is observed to be compatible with the experimental and computational trends.

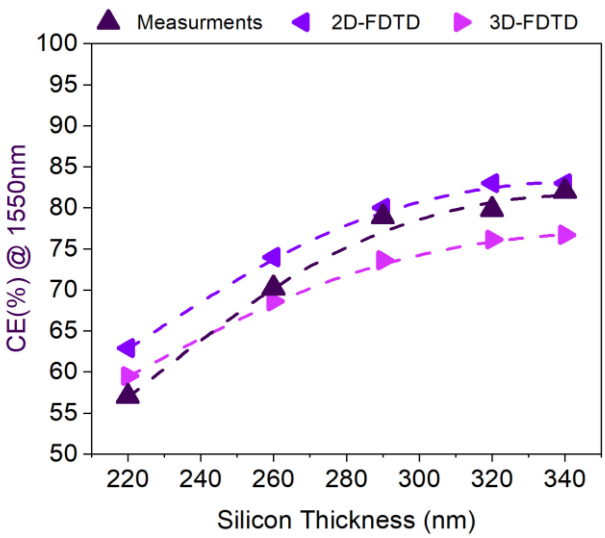

Fig. 3. Comparison of the measured best Coupling-Efficiencies (CEs) at 1550 nm for the five different Silicon-on-Insulator (SOI) thicknesses with the 2D- and 3D-FDTD simulated values. The dashed line refers to a second order polynomial fit of the CEs.

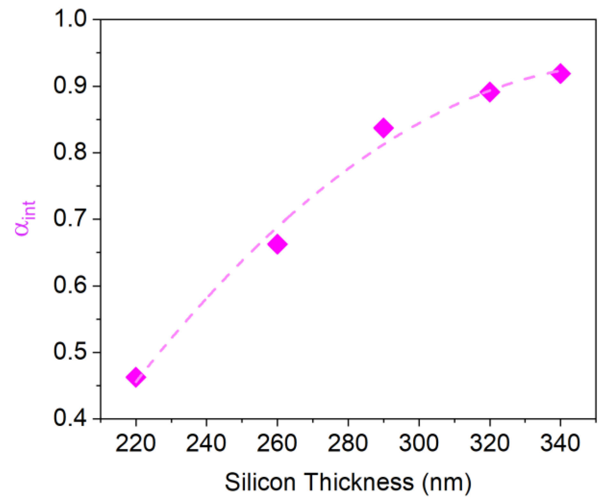

Fig. 4. Spatial integrated leakage factor (α_{int}) estimated with 2D-FDTD simulations at 1550 nm for different SOI thicknesses referred to GCs optimized for the H-Fb scheme. The dash line indicates a second order polynomial fit of the α_{int} values.

The multi-wavelength CEs, either measured and computational, for each SOI thickness are reported in supplementary material Fig. S8. Moreover, the measured 1dB bandwidths are summarized in supplementary material Table S2.

Now to deeper understand the GC operational behavior, it is important to be aware of the physics behind the CE, thus the scattering process for each structure has been analyzed considering its dependence from two specific features: the directionality (D) and the reflectivity (R) [5]. It is important to underline that both D and R are exclusively related to the structural parameters and together with the MFD of the source define the coupling performances.

We introduce the leakage factor (α) as a physical variable to investigate D. For non-uniform GC α is a function of the position along X, which is the direction of apodization of the local pitches, and the tuning-wavelength λ_c, equal to 1550 nm in our analysis,

$$2\alpha(X, \lambda_c) = \frac{I^2(X, \lambda_c)}{I_0^2(\lambda_c) - \int_x^x I^2(t, \lambda_c)dt} \tag{3}$$

where $I^2(X)$ is the leakage power intensity evaluated point by point, I_0^2 is the initial power intensity coming from the injection medium [25]. Usually, the α parameter is employed to optimize ED and FF in order to reshape the power profile emission of a non-uniform GC to make it Gaussian [26]. As a consequence, α affects also the D of a non-uniform GC and, thus, it has been implemented in the analysis because directly related to the structural features.

An easy approach to evaluate α is to consider the GC in the out-coupling configuration. To perform a quantitative comparison of the scattering strengths across the SOI thicknesses, the spatial integral of $\alpha(X)$ along the apodization direction has to be evaluated. This is a new parameter in the framework of the non-uniform GC optimization and for consistency is called α_{int}. The α_{int} values for the SOIs under investigation are plotted in Fig. 4.

It can be noticed that α_{int} increases monotonically along the Silicon thicknesses with a constant decreasing in the slope showing a trend that is compatible with a quadratic fit.

Therefore, not only a greater directionality for higher SOI layers is expected, but more generally a superior ability in diffracting in- and out- the incoming light. In particular, it is interesting to highlight that the trends reported in Fig. 3 related to CEs and in Fig. 4 for the α_{int} are similar suggesting the important role of the scattering strength in defining the performance of the GCs.

Instead, the R is investigated through the effective refractive index, which is a function of the position along the apodization direction X, and is responsible for the impedance matching. A photonic band structure approach [27] has been considered to evaluate these quantities going beyond the n_{eff}^{AVG} calculation, implemented in the design procedure. Assuming that a non-uniform GC can be considered as a series of pitch junctions [28], the effective refractive index has been calculated for each structure selecting proper P_i, where i indexes the pitch number, scanning the entire GC length [29]. The corresponding results, indicated as n_{eff}^{BS}, are displayed in Fig. 5 showing a monotonic decrease across the periods.

These linear trends suggest that the linear apodization of FF, which is a structural parameter, turn into a non-trivial linear impedance matching, that is a property related to the electromagnetic field. For the sake of completeness, the variations of the FF and the corresponding local pitches are reported in supplementary material section 2 Fig. S2 displaying a linear behavior as expected. Fig. 5 enables a direct comparison between the slope of each linear fit. The n_{eff}^{BS} is a function of the ED and the ratio of the ED to the SOI thickness tends to increase for higher silicon thicknesses leading to a greater difference between the waveguide impedance and the impedance of the contiguous local pitch. Thus, the slope of the trends has to be greater moving

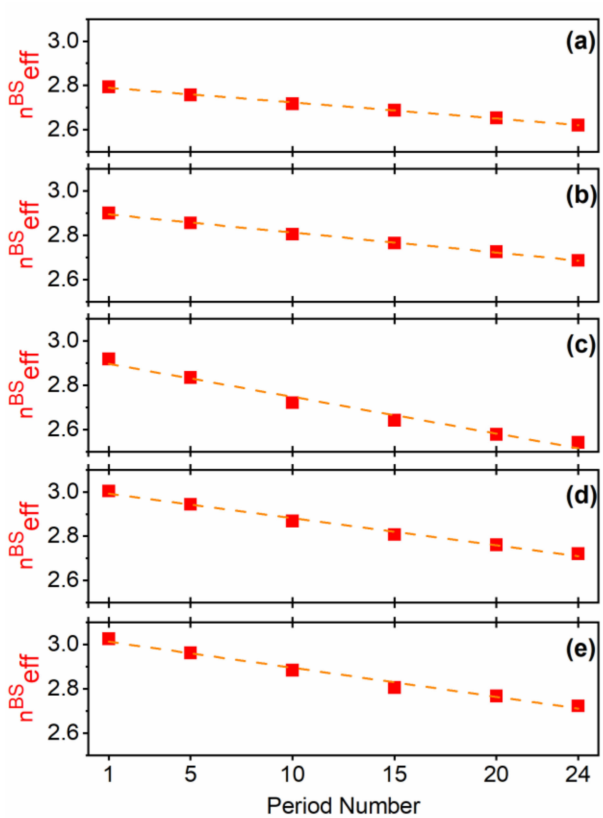

Fig. 5. Variation of the effective refractive index at 1550 nm as a function of the period number calculated resorting to a band structure approach. The dashed line refers to a linear fit of the n_{eff}^{BS}. (a) 200 nm-thick SOI, (b) 260 nm-thick SOI, (c) 290 nm-thick SOI, (d) 320 nm-thick SOI, and (e) 340 nm-thick SOI.

towards thicker SOI to close the gap in the impedance matching for an equal number of periods. The 290 nm SOI shows a trend slightly different respect to the other suggesting that a further investigation might be considered. In addition, assuming a linear variation of the n_{eff}^{BS}, an average slope value of 0.013 has been calculated showing a smoother apodization parameter of the n_{eff}^{BS} compared to the linear apodization of the FF across the P_i, where an average slope of 0.017 has been evaluated. This shows the ability of the GC in reducing the R boosting consequently the CE.

An experimental estimation of the R around λc was performed, following the procedure reported in [30], with values of approximately 0.3%, 0.2%, 0.5%, 0.2%, and 0.4% for respectively the 220 nm-, 260 nm-, 290 nm-, 320 nm-, and 340 nm-thick SOI. A computational evaluation of R was also done exploiting 2D-FDTD simulations to have a feedback on the experimental results on a spectral interval of about 100 nm. The corresponding results are summarized in supplementary material section 2 Fig S5. In particular, R can be further improved independently of the SOI thickness exploiting more complex designs based on two-step-etching subwavelength GCs, as it has been reported in [30]–[35].

For the sake of completeness, a computational estimation of the optical power ratio (OPR) at λ_c for the power scattered upward (OPR_U), downward (OPR_D), backward (OPR_B), and forward (OPR_F) to the input optical power is reported in supplementary material section 2 for each SOI thickness.

In order to highlight the increment of the ED as a function of the SOI, the corresponding data are reported in supplementary material section 2 Fig. S3.

A check of the structural parameters of the first and last P_i using the SEM technique was provided by the foundry resulting in low discrepancies of the geometrical features and the computational requirements, see supplementary material for more information regarding the fabrication tolerances. Additional SEM measurements have been performed on a previously optically characterized sample with a 260 nm-thick SOI to evaluate all the P_i.

The corresponding SEM image related to this sample can be found in supplementary material section 2 Fig. S7.

Then, the results have been imported inside the FDTD software to evaluate the CE. This specific GC was chosen considering the trend of α_{int} depicted in Fig. 4. The plot can be approximatively divided into two parts characterized by a different incremental variation: a lower part with a fast α_{int} increasing composed by the 220 nm-thick platform, 260 nm-thick and 290 nm-thick SOIs, and an upper part containing the 290 nm-, 320 nm-, and 340 nm-thick SOIs with similar α_{int} values flattening the curve. As a consequence, the disagreement between each theoretical α_{int} value and the corresponding real one is more sensitive, in the lower part, to a discrepancy in the P_i resulting in a lower CE. Due to this consideration, the lower section is observed to be the most critical in terms of the D and the 260 nm-thick SOI has been chosen being its midpoint. The P_i were measured and plotted, showing a linear trend in agreement with the computational expectations. The comparison of the measured and simulated fit parameters shows a good agreement within a 0.1% difference in the slope values. This demonstrates that the actual apodization trend mimics well the apodization function. Finally, the measured local pitches were used to re-build the corresponding non-uniform GCs inside a 2D- and 3D-FDTD to check the computational performances and in both cases a discrepancy of less than 1% respect to the corresponding optimized structure were calculated.

IV. Conclusion

In this work, we report the first experimental characterization of focusing non-uniform GCs designed on different SOI thicknesses (220 nm, 260 nm, 290 nm, 320 nm, and 340 nm) for the horizontal-fiber light-coupling scheme. An overall best CE of 83% has been measured for the 340 nm-thick SOI, which is the highest measured value reported in literature for this coupling scheme. Incidentally, the best measured CEs for both the 220 nm-thick and the 340 nm-thick standard platforms shows competitiveness with the corresponding values of the more established vertical-fiber light-coupling scheme reported in literature. The behavior of the best experimental CEs as a function of the SOI thickness has been observed to be compatible with a quadratic fit performing systematic measurements on multiple samples of the same structure. The nature of the variation of the CE has been studied and explained through a new scattering parameter called integrated leakage factor (α_{int}) defined for the first time for non-uniform GCs. The α_{int} variation displays the same behavior of the CEs suggesting a quadric increment also in the directionality and so in the power scattered in and out by the GCs. Finally, we studied the effect of the linear apodization function on the propagation of the light for all the SOI thicknesses. In particular, the evolution of the effective refractive index n_{eff}^{BS}, calculated using a photonic bandstructure analysis, as a function of the periods indicates that a linear apodization turns into a linear impedance matching. Furthermore, we strongly believe that the proposed procedure can represent an improvement for the comprehension of the light scattering phenomena as complex as in grating coupling.

Acknowledgment

The authors would like to thank Dr. Lee Carroll for the fruitful discussion and the significant support offered during the paper preparation and Simone Iadanza for collecting the SEM images.

References

[1] R. Soref, "Silicon photonics: A review of recent literature," *Silicon*, vol. 2, pp. 1–6, Jan. 2010.

[2] Z. Fang, and C. Z. Zhao, "Recent progress in silicon photonics: A review," *ISRN Opt.*, vol. 2012, pp. 1–28, Mar. 2012.

[3] A. E. Lim *et al.*, "Review of silicon photonics foundry efforts," *IEEE J. Sel. Top. Quant. Electron*, vol. 20, no. 4, pp. 405–416, Jul./Aug. 2014, Art no. 8300112.

[4] L. Tsybeskov, D. J. Lockwood, and M. Ichikawa, "Silicon photonics: CMOS going optical [Scanning the Issue]," in *Proc. IEEE*, vol. 97, no. 7, pp. 1161–1165, Jul. 2009.

[5] R. Marchetti, C. Lacava, L. Carroll, K. Gradkowski, and P. Minzioni, "Coupling strategies for silicon photonics integrated chips," *Photon. Res.*, vol. 7, no. 2, pp. 201–239, Feb. 2019.

[6] L. Cheng, S. Mao, Z. Li, Y. Han, and H. Y. Fu, "Grating couplers on silicon photonics: Design principles, emerging trends and practical issues," *Micromachines*, vol. 11, no. 7, pp. 666, Jul. 2020.

[7] D. Taillaert *et al.*, "Grating couplers for coupling between optical fibers and nanophotonic waveguides," *Jpn. J. Appl. Phy.*, vol. 45, pp. 6071–6077, Aug. 2006.

[8] D. Vermeulen *et al.*, "High-efficiency fiber-to-chip grating couplers realized using an advanced CMOS-compatible silicon-on-insulator platform," *Opt. Exp.*, vol. 18, no. 17, pp. 18278–18283, 2010.

[9] F. Van Laere *et al.*, "Compact and highly efficient grating couplers between optical fiber and nanophotonic waveguides," *J. Light. Technol.*, vol. 25, no. 1, pp. 151–156, 2007.

[10] S. K. Selvaraja *et al.*, "Highly efficient grating coupler between optical fiber and silicon photonic circuit," in *Proc. Conf. Lasers Electro-Opt./Int. Quant. Electron. Conf.*, CTuC6, Jun. 2009.

[11] A. Bozzola, L. Carroll, D. Gerace, I. Cristiani, and L. C. Andreani, "Optimising apodized grating couplers in a pure SOI platform to −0.5 decibels coupling efficiency," *Opt. Exp.*, vol. 23, no. 12, pp. 16289–16304, Jun. 2015.

[12] R. Marchetti *et al.*, "High-efficiency grating-couplers: Demonstration of a new design strategy," *Sci. Rep.*, vol. 7, Nov. 2017, Art. no. 16670.

[13] L. He *et al.*, "A high-efficiency nonuniform grating coupler realized with 248-nm optical lithography," *IEEE PTL*, vol. 25, no. 14, pp. 1358–1361, Jul. 2013.

[14] X. Chen, C. Li, C. K. Y. Fung, S. M. G. Lo, and H. K. Tsang, "Apodized waveguide grating couplers for efficient coupling to optical fibers," *IEEE PTL*, vol. 22, no. 15, pp. 1156–1158, Aug. 2010.

[15] C. Li, K. S. Chee, J. Tao, H. Zhang, M. Yu, and G. Q. Lo, "Silicon photonics packaging with lateral fiber coupling to apodized grating coupler embedded circuit," *Opt. Exp.*, vol. 22, no. 10, pp. 24235–24240, Oct. 2014.

[16] S. Li *et al.*, "Deterministic design of focusing apodized subwavelength grating coupler based on weak form and transformation optics," *Opt. Exp.*, vol. 28, no. 23, pp. 35395–35412, Nov. 2020.

[17] M. H. Lee, J. Y. Jo, D. W. Kim, Y. Kim, and K. H. Kim, "Comparative study of uniform and nonuniform grating couplers for optimized fiber coupling to silicon waveguides," *J. Opt. Soc. Korea*, vol. 20, no. 2, pp. 291–299, Apr. 2016.

[18] L. Carroll *et al.*, "Photonic packaging: Transforming silicon photonic integrated circuits into photonic devices," *Appl. Sci.*, vol. 6, no. 12, p. 426, Dec. 2016.

[19] M. Passoni *et al.*, "Co-optimizing grating couplers for hybrid integration of InP and SOI photonic platforms," *AIP Adv,* vol. 8, no. 9, Sep. 2018, Art. no. 095109.

[20] Lumerical Inc., [Online]. Available: http://www.lumerical.com/tcad-products/fdtd/

[21] J. Robinson, and Y. Rahmat-Samii, "Particle swarm optimization in electromagnetics," *IEEE Trans. Antennas Propag.*, vol. 52, no. 2, pp. 397–407, Feb. 2004.

[22] L. Zagaglia, F. Floris, and P. O'Brien, "Optimized design procedure for Low-cost Grating-couplers in Photonics-packaging," in *Proc. Photon. Electromagnetics Res. Symp. - Spring*, 2019, pp. 234–241.

[23] F. Van Laere *et al.*, "Compact focusing grating couplers for Silicon-on-Insulator integrated circuits," *IEEE PTL*, vol. 19, no. 23, pp. 1919–1921, Dec. 2007.

[24] Cornerstone, [Online]. Available: https://www.cornerstone.sotonfab.co.uk

[25] R. Waldhäusl, B. Schnabel, P. Dannberg, E. B. Kley, A. Bräuer, and W. Karthe, "Efficient coupling into polymer waveguides by gratings," *Appl. Opt.*, vol. 36, no. 36, pp. 9383–9390, Dec. 1997.

[26] Z. Zhao, and F. Shanhui, "Design principles of apodized grating couplers," *J. Lightw. Technol.*, vol. 38, no. 16, pp. 4435–4446, Feb. 2020.

[27] J. D. Joannopoulos, S. G. Johnson, J. N. Winn, and R. D. Meade, *Photonic Crystals: Molding the Flow of Light*, 2nd ed., NJ: Princeton Univ. Press, 2008.

[28] S. G. Johnson, P. Bienstman, M. A. Skorobogatiy, M. Ibanescu, E. Lidorikis, and J. D. Joannopoulos, "Adiabatic theorem and continuous coupled-mode theory for efficient taper transitions in photonic crystals," *Phys. Rev. E*, vol. 66, no. 6, Dec. 2002, Art. no. 066608.

[29] L. Zagaglia, F. Floris, and P. O'Brien, "Analysis in reciprocal space of the band-pass filter effect in uniform and non-uniform grating couplers," *J. Phys. Conf. Ser.*, vol. 1548, Jul. 2019, Art. no. 012031.

[30] D. Benedikovic *et al.*, "L-shaped fiber-chip grating couplers with high directionality and low reflectivity fabricated with deep-UV lithography," *Opt. Lett.*, vol. 42, no. 17, pp. 3439–3442, 2017.

[31] D. Benedikovic *et al.*, "Sub-decibel silicon grating couplers based on L-shaped waveguides and engineered subwavelength metamaterials," *Opt. Exp.*, vol. 27, no. 18, pp. 26239–26250, Sep. 2019.

[32] T. Watanabe, M. Ayata, U. Koch, Y. Fedoryshyn, and J. Leuthold, "Perpendicular grating coupler based on a blazed antiback-reflection structure," *J. Light. Technol.*, vol. 35, no. 21, pp. 4663–4669, Nov. 2017.

[33] D. Melati *et al.*, "Mapping the global design space of nanophotonic components using machine learning pattern recognition," *Nat Commun*, vol. 10, Oct. 2019, Art. no. 4775.

[34] M.K. Dezfouli *et al.*, "Perfectly vertical surface grating couplers using subwavelength engineering for increased feature sizes," *Opt. Lett.*, vol. 45, no. 13, pp. 3701–3704, May 2020.

Luca Zagaglia received the bachelor's and the master's degree in physics, curricula of matter physics from the University of Pavia, Pavia, Italy. In 2017, he joined Tyndall National Institute, Cork, Ireland, as a Ph.D. Student with Photonics Packaging Group. His research is mainly focused on optimization, modelling and developing new coupling schemes for integrated photonic devices. He developed hard skills in computational methods based on finite-different time domain, ray tracing, and wave optics.

Francesco Floris received the bachelor's degree in physics from the University of Cagliari, Cagliari, Italy, and the master's degree in physics, curricula of matter physics and the Ph.D. degree in physics from the University of Pavia, Pavia, Italy. During the Ph.D. degree, he was a Research Scholar with Boston University, Boston, MA, USA. He was with the University of Cagliari, Cagliari, Italy, as didactical Tutor, teaching physics and mathematics in bachelor's and master's classes. In 2017, he joined Tyndall National Institute, Cork, Ireland, and is currently Research Manager with Photonics Packaging Group. His research focuses on the development and optimization of optical coupling schemes for optoelectronic devices. His hard skills span from spectroscopic and microscopy techniques to computational models based on the finite-difference time-domain method. He was the recipient of Exchange Programme Prize of the Italian Ministry of Education, Universities and Research.

Peter A. O'Brien received a degree in physics and the master's degree in electronic engineering from Trinity College Dublin, Dublin, Ireland, and the Ph.D. degree in physics from University College Cork, Cork, Ireland. He was a Postdoctoral Scholar with the California Institute of Technology, Pasadena, CA, USA and a Research Scientist with the NASA's Jet Propulsion Laboratory (Micro Devices Laboratory), La Cañada Flintridge, CA, USA. In 2006, he founded Epi-Light limited, a photonics company specializing in the development of advanced imaging systems for biotechnology and medical device applications. After selling his company, he joined the Tyndall Institute, Cork, Ireland, where he is currently the Head of the Photonics Packaging Group and is responsible for a wide range of both academic and industry research projects, across the telecoms and medical device sectors. His group is also involved in a large number of major EU collaborative projects in the area of silicon photonics. In all these projects, his group leads the packaging and integration activities.